Available online at www.elixirpublishers.com (Elixir International Journal)

Organic Chemistry

Elixir Org. Chem. 73A (2014) 26581-26588

ISSN: 2229-712X

Vibrational analysis of 2-chloro-1-fluoro-4-nitrobenzene a joint FT-IR, FT-Raman and Scaled Quantum Chemical Study

P.Vennila[1,*], M.Govindaraju[2] and G.Venkatesh[3]

[1]Research and Development Centre, Bharathiar University, Coimbatore - 641 046, India.

[2]Department of Chemistry, Kongu Polytechnic College, Erode- 638052, India.

[3]Department of Chemistry, VSA Group of Institutions, Salem, Tamilnadu, India.

ARTICLE INFO

Article history:

Received: 16 June 2014;

Received in revised form:

18 August 2014;

Accepted: 27 August 2014;

Keywords

Density Functional Theory,
FT-Raman, FT-IR, HOMO,
LUMO, NBO,
First-order Hyperpolarizability,
Electronic Excitation Energy.

ABSTRACT

Vibrational spectral analysis was carried out for 2-chloro-1-fluoro-4-nitrobenzene (CFNB) by using the FT-IR and FT-Raman spectroscopy in the range of 4000 cm^{-1} to 400 cm^{-1} and 4000 cm^{-1} to 100 cm^{-1} respectively. The theoretical computational density functional theory (DFT/B3LYP) was performed at 6-311+G** levels to derive equilibrium geometry, vibrational wavenumbers, infrared intensities and Raman scattering activities. The complete vibrational assignment was performed on the basis of the total energy distribution (TED), calculated with scaled quantum mechanics (SQM) method. Natural bond orbital (NBO) analysis was applied to study stability of the molecule arising from charge delocalization. Quantum chemical parameters such as the highest occupied molecular orbital energy (HOMO), the lowest unoccupied molecular orbital energy (LUMO), energy gap (ΔE), were calculated.

Introduction

2-chloro-1-fluoro-4-nitrobenzene [CFNB] is also used in shoe and floor polishes, leather dressings, paint solvents, and other materials to mask unpleasant odors. Redistilled, as oil of mirbane, CFNB has been used as an inexpensive perfume for soaps [1,2]. A significant merchant market for CFNB used in the production of the analgesic paracetamol (also known as acetaminophen), used in Kerr cells, as it has an unusually large Kerr constant and used as an intermediate for organic compounds; pharmaceuticsals, pesticides and dyes.

FT-IR and FT-Raman spectra of CFNB have been recorded in the regions 4000-400 cm^{-1} and 4000-100 cm^{-1}. Hence, the present work has been undertaken to give a complete description of the molecular geometry and molecular vibrations of the title compound. The complete vibrational analysis of CFNB was performed by combining the experimental and theoretical information using DFT based scaled quantum chemical approach.

Experimental Details

The compound CFNB was obtained from Lancaster Chemical Company, UK and used as such for the spectral measurements. The room temperature Fourier Transform infrared spectrum of the title compound was measured with KBr pellet technique in the 4000-400 cm^{-1} region at a resolution of 1 cm^{-1} using BRUKER IFS 66V spectrophotometer equipped with He-Ne laser source. The FT-Raman spectrum of CFNB was recorded on a BRUKER IFS-66V model interferometer equipped with an FRA-106 FT-Raman accessory in the 4000-100 cm^{-1} stoke region using the 1064 nm line of a Nd:YAG Laser for excitation operating at 200mW power. The reported wave numbers are believed to be accurate within ±1 cm^{-1}.

Computational Details

The entire quantum chemical calculations have performed at B3LYP/ 6-31G** and B3LYP/6-311+G** basis sets using the GAUSSIAN 09W program package [3].The optimized structural parameters have been evaluated for the calculation of vibrational frequencies at Becke's three parameter hybrid model using the Lee-Yang-Parr [4,5] correlation functional (B3LYP) method by assuming C_s point group symmetry. As a result, the unscaled calculated frequencies reduced mass, force constant, infrared intensity and Raman activity, are obtained. In order to fit the theoretical frequencies to the experimental frequencies, an overall scaling factor has been introduced by using a least-square optimization of the computed to the experimental data. The assignments of the calculated normal modes have been made on the basis of the corresponding TEDs. The TEDs are computed from quantum chemically calculated vibrational frequencies using MOLVIB program version 7.0 written by Sundius [6]. Gauss view program [7] has been considered to get visual animation and also for the verification of the normal modes assignment.

The prediction of Raman intensities

The prediction of Raman intensities was carried out by following the procedure outlined below. The Raman activities (*Si*) calculated by the GAUSSIAN 09W program are adjusted during scaling procedure with MOLVIB were converted to relative Raman intensities (*Ii*) using the following relationship derived from the basic theory of Raman scattering [8-9].

$$I_i = \frac{f(v_o - v_i)^4 S_i}{v_i[1-\exp(-hcv_i / KT)} \quad \text{----------(1)}$$

Where υ_0 is the exciting frequency (in cm^{-1}), υ_i is the vibrational wavenumber of the normal mode; h, c and k are universal constants, and f is a suitably chosen common normalization factor for all peak intensities.

Results and discussion

Geometrical parameters

In order to find the most optimized geometry, the energy calculations were carried out for CFNB, using B3LYP/6-311+G** basis set for various possible conformers. The

Tele: +91-9788593970
E-mail addresses: vennilaindhu84@gmail.com

optimized molecular structure of CFNB is shown in Fig 1. The total energies obtained for B3LYP/6-311+G** are listed in Table 1. The most optimized structural parameters were also calculated and they were depicted in Table 2.

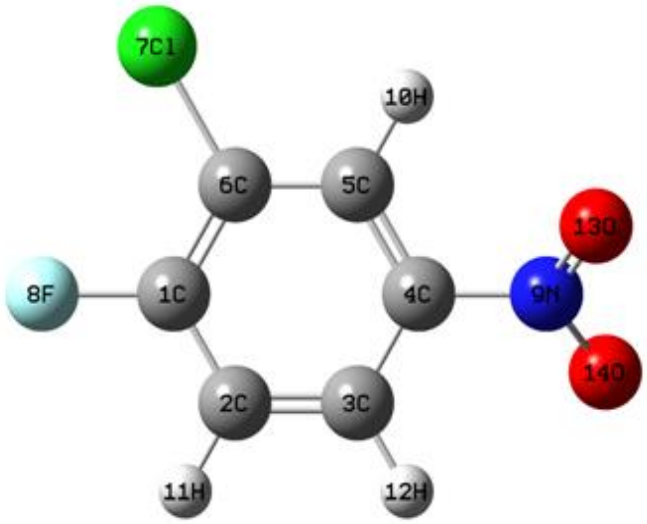

Fig 1. The optimized molecular structure of CFNB

Table1. Total energies of CFNB, calculated at DFT B3LYP/6-31G* and B3LYP/6-311+G level**

Method	Energies (Hartrees)
6-31G*	-995.35648921
6-311+G**	-995.57281237

Table 2. Optimized geometrical parameters of CFNB obtained by B3LYP/6–311+G density functional calculations**

Bond length	Value(Å)	Bond angle	Value(Å)	Dihedral angle	Value(Å)
C2-C1	1.38599	C3-C2-C1	120.00023	C4-C3-C2-C1	0.00000
C3-C2	1.38600	C4-C3-C2	120.00023	C5-C4-C3-C2	0.00000
C4-C3	1.38599	C5-C4-C3	120.00160	C6-C5-C4-C3	0.00000
C5-C4	1.38607	C6-C5-C4	119.99816	Cl7-C6-C5-C4	179.42860
C6-C5	1.38600	Cl7-C6-C5	120.00047	F8-C1-C2-C3	179.42728
Cl7-C6	1.75997	F8-C1-C2	119.99899	N9-C4-C3-C2	179.42810
F8-C1	1.49005	N9-C4-C3	119.99899	H10-C5-C4-C3	179.42801
N9-C4	1.44605	H10-C5-C4	119.99854	H11-C2-C1-C6	179.42803
H10-C5	1.12197	H11-C2-C1	119.99647	H12-C3-C2-C1	179.42805
H11-C2	1.12197	H12-C3-C2	120.00081	O13-N9-C4-C3	-139.42577
H12-C3	1.12197	O13-N9-C4	119.99470	O14-N9-C4-C3	41.14849
O13-N9	1.13178	O14-N9-C4	119.99996		
O14-N9	1.31596				

*for numbering of atom refer Fig 1

Vibrational frequencies and normal coordinate analysis

The optimized structural parameter were used to compute the vibrational frequencies of CFNB at B3LYP/6-311+G** level of calculations. The molecule belongs to C_s point group symmetry. The CFNB molecule under investigation has 14 atoms give rise to 36 normal modes of fundamental vibrations, which span the irreducible representations: 25 A'+11 A", all the 36 fundamental vibrations are active in both IR and Raman.

Normal coordinate analysis was carried out to provide a complete assignment of the fundamental vibrational frequencies for the molecule. For this purpose, the full set of 49 standard internal coordinates containing 13 redundancies for CFNB were defined as given in Table 3. From these, a non-redundant set of local symmetry coordinates were constructed by suitable linear combinations of internal coordinates following the recommendations of Puley et al.[10] and they were presented in Table 4. The theoretically calculated DFT force fields were transformed to this later set of vibrational coordinates and used in all subsequent calculations. The observed FT-IR and FT Raman spectra of the title compound were presented in Fig 2 and Fig 3, respectively which helps to understand the observed spectral frequencies. The detailed vibrational assignments of fundamental modes of CFNB along with calculated IR, Raman intensities and normal mode descriptions (characterized by TED) were reported in Table 5.

Root mean square (RMS) values of frequencies were obtained in the study using the following expression,

$$RMS = \sqrt{\frac{1}{n-1}\sum_{i}^{n}\left(\upsilon_i^{calc} - \upsilon_i^{exp}\right)^2}$$

The RMS error of the observed and calculated frequencies (unscaled / B3LYP/6-311+G**) of CFNB was found to be 105 cm^{-1}. This is quite obvious; since the frequencies calculated on the basis of quantum mechanical force fields usually differ appreciably from observed frequencies.

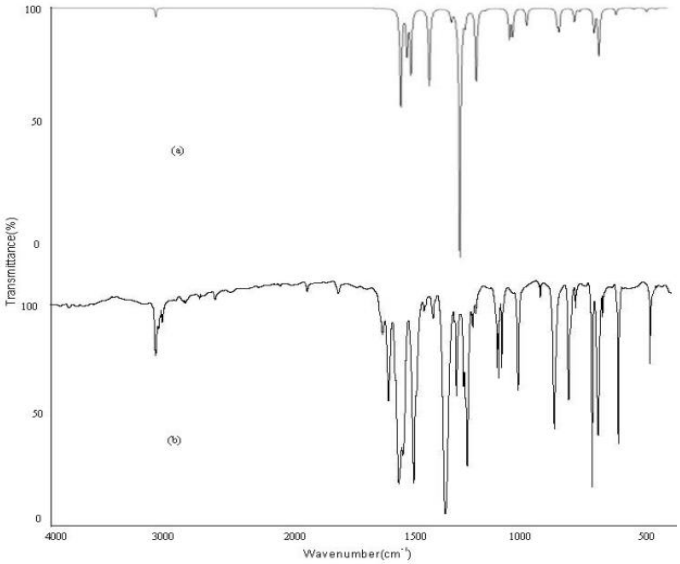

Fig 2. FT-IR spectra of CFNB
(a)Calculated (b) Observed with B3LYP/6-311+G**

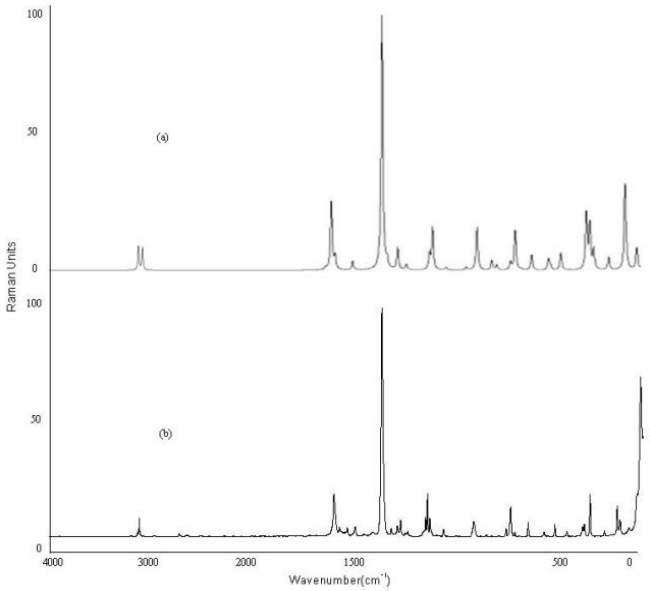

Fig 3. FT-Raman spectra of CFNB
(a) Calculated (b) Observed with B3LYP/6-311+G**

This is partly due to the neglect of anharmonicity and partly due to the approximate nature of the quantum mechanical methods. In order to reduce the overall deviation between the unscaled and observed fundamental frequencies, scale factors were applied in the normal coordinate analysis and the

subsequent least square fit refinement algorithm resulted into a very close agreement between the observed fundamentals and the scaled frequencies. Refinement of the scaling factors applied in this study achieved a weighted mean deviation of 7.51 cm^{-1} between the experimental and scaled frequencies of the title compound.

C–H vibrations

For simplicity, modes of vibrations of aromatic compounds are considered as separate C−H vibrations. Substituted benzenes have large number of sensitive bands, i.e., bands whose position is significantly affected by the mass and electronic properties, mesomeric or inductive of the substituents. According to the literature [11], in infrared spectra, most aromatic compounds have three or four peaks in the region 3300–3100 cm^{-1}, these are due to the stretching vibrations of the ring CH bands. Accordingly, in the present study, the FT-IR bands identified at 3275, 3274, 3247, 3245 and 3243 cm^{-1} and FT Raman bands at 3277, 3276 and 3273 cm^{-1} are assigned to C–H stretching vibrations of CFNB which are in good agreement with calculated values by B3LYP/6-311+G**. The FT-IR bands at 1546, 1545, 1441, 1440 and 1439 cm^{-1} and the FT Raman bands at 1442, 1440 and 1439 cm^{-1} are assigned to C–H in-plane bending vibration of CFNB. The C–H out-of-plane bending vibrations of the CFNB are well indentified at 1278 and 1276 cm^{-1} in the FT IR and 1165, 1162 and 1159 cm^{-1} in the FT-Raman spectra which are found to be well within their characteristic region.

C-C vibrations

The ring C–C stretching vibrations, usually occur in the region 1680–1450 cm^{-1} [12]. Hence in the present investigation, the FT-IR bands indentified at 1659, 1655, 1653, 1546, 1545, 1441 and 1440 cm^{-1} and the FT-Raman bands at 1638, 1636, 1633, 1442 and 1439 cm^{-1} are assigned to C–C stretching vibrations of CFNB. The band ascribed at 828, 824 and 821 cm^{-1} in FT-IR and 732, 729 and 721 cm^{-1} in FT-Raman spectra has been designated to C-C in-plane and out-of-plane bending mode.

Ring vibrations

Several ring modes are affected by the substitution to the aromatic ring of CFNB. In the present study, the bands ascribed at 978, 976, 935, 932, 929, 926, 920, 828, 824, 821, 756, 748, 752, 732, 729, 721 and 700 cm^{-1} for CFNB have been designated to ring in-plane and out-of-plane bending modes, respectively, by careful consideration of their quantitative descriptions. A small change in frequency observed for these modes are due to the changes in force constant/reduced mass ratio.

C-N vibrations

The IR and Raman bands appeared at 1441, 1439 cm^{-1} and 1442, 1440 cm^{-1} in CFNB have been designated to C-N stretching vibrations respectively. The in-plane and out-of-plane bending vibrations are observed at 1148, 1146, 1144, 935, 932, 929, 926 and 920 cm^{-1} in this study are also supported by the literature [13,14]. The identification of C-N vibration is a difficult task since, it falls in a complicated region of the vibrational spectrum. However, with the help of force field calculations, the C-N vibrations were identified and assigned in this study.

Nitro group vibrations

The characteristics group frequencies of nitro group are relatively independent of the rest of the molecule, which makes this group convenient to identify. Nitro compounds have strong absorptions due to the asymmetric and symmetric stretching vibrations of the NO_2 group at 1680–1485 cm^{-1} and 1390-1320 cm^{-1}, respectively [15]. The infrared and Raman band observed at 1685, 1682 cm^{-1} and 1638, 1636, 1633 cm^{-1} have been designated to asymmetric and symmetric stretching modes of NO_2 group, respectively. The scissoring modes of NO_2 group have been designated to the band at 732, 729 and 721 cm^{-1} in Raman. The band at 372 cm^{-1} in Raman is attributed to NO_2 rocking mode. The bands observed at 356 and 354 cm^{-1} have been designated to NO_2 wagging and NO_2 twisting modes, respectively.

C-F vibrations

The vibrations belonging to the bond between the ring and the halogen atoms are worth to discuss here, since mixing of vibrations is possible due to the presence of heavy atoms on the molecule [16]. In CFNB, the C−F stretching vibrations appeared at 1659, 1655, 1653, 1546 and 1545 cm^{-1} in FT-IR and 1325, 1322 and 1319 cm^{-1} in FT-Raman spectra. The C−F in-plane bending vibrations were found at 828, 824, 821, 702, 700, 697 cm^{-1} and 850, 848, 846,732, 729, 721 cm^{-1} in FT IR and FT-Raman spectrum. The C−F out-of-plane bending mode is recorded at 568, 564, 561, and 459 cm^{-1} in FT-IR. The calculated values of C−F stretching, in-plane bending and out of-plane bending modes are found to be at 337, 334, 332, 261 and 259 cm^{-1}.

C–Cl vibrations

In the present investigation C–Cl stretching vibrations observed at 568, 564 and 561 cm^{-1}. The ring halogen stretching mode were observed as strong Raman and weak to medium IR bands at 850–560 cm^{-1} range for chlorine [17]. As expected in our studies, the bands at 558, 554 and 550 cm^{-1} are assigned to C–Cl stretching vibration with ring deformation vibration.

NBO Analysis

The NBO analysis is an effective tool for interpretation of intra- and intermolecular interaction; it also provides a convenient basis for investigating charge transfer or conjugative interaction in molecular system. The larger the E(2) (energy of hyper conjugative interactions) value, the more intensive is the interaction between electron donors and electron acceptors, i.e. the more donating tendency from electron donors to electron acceptors, the greater the extent of conjugation of the whole system. Delocalization of electron density between occupied Lewis-type (bond or lone pair) NBO orbitals and formally unoccupied (anti-bond or Rydgberg) non-Lewis NBO orbitals correspond to a stabilizing donor–acceptor interaction. NBO analysis has been performed on the title molecule at the DFT/B3LYP/6-311+G** level in order to explain the intra molecular, re-hybridization and delocalization of electron density within the molecule. The results of second order perturbation theory analysis of Fock matrix collected in Table 6 indicate the intra-molecular interactions due to the orbital overlap of π(C2-C3) over antibonding π*(C1-C6) with energies 23.88 kcal/mol, π(C1-C6) over π*(C2-C3) and π*(C4-C5) with stabilization energies 17.31 kcal/mol and 21.60 kcal/mol. The most important interactions in the title molecule having lonepair O13 and O14 with that of antibonding π*(N9-O13) and σ*(N9-O14) results to the stabilization of 93.0 kcal/mol and 30.2 kcal/mol.

First-order hyperpolarizability calculations

The first-order hyperpolarizabilities (β_0) of this novel molecular system, and related properties β_0, α_0 and $\Delta\alpha$) of CFNB were calculated using B3LYP/6-311+G** basis set, based on the finite-field approach. In the presence of an applied electric field, the energy of a system is a function of the electric field. First-order hyperpolarizability is a third rank tensor that can be described by 3×3×3 matrix.

Table 3. Definition of internal coordinates of CFNB

No(i)	symbol	Type	Definition
Stretching 1-6	r_i	C-C	C1-C2,C2-C3,C3-C4,C4-C5,C5-C6,C6-C1
7-9	S_i	C-H	C2-H11,C3-H12,C5-H10
10	p_i	C-F	C1-F8
11	P_i	C-Cl	C6-Cl7
12	N_i	C-N	C4-N9
13-14	$\sum_i$	N-O	N9-O13,N9-O14
Bending 15-20	α_i	C-C-C	C1-C2-C3,C2-C3-C4,C3-C4-C5, C4-C5-C6,C5-C6-C1,C6-C1-C2
21-26	θ_i	C-C-H	C1-C2-H11,C3-C2-H11,C2-C3-H12, C4-C3-H12,C4-C5-H10,C6-C5-H10
27-28	β_i	C-C-F	C6-C1-F8, C2-C1-F8
29-30	Φ_i	C-C-Cl	C5-C6-Cl7, C1-C6-Cl7
31-32	μ_i	C-C-N	C3-C4-N9, C5-C4-N9
33-34	γ_i	C-N-O	C4-N9-O13, C4-N9-O14
35	ν_i	O-N-O	O13-N9-O14
Out-of-plane 36-38	ω_i	C-H	H11-C2-C1-C3, H12-C3-C2-C4, H10-C5-C4-C6
39	ξ_i	C-F	F8-C1-C2-C6
40	Ω_i	C-Cl	Cl7-C6-C1-C5
41	ε_i	C-N-O	C4-N9-O13-O14
42	ι_i	C-N	N9-C4-C3-C5
Torsion43-48	τ_i	C-C	C1-C2-C3-C4,C2-C3-C4-C5,C3-C4-C5-C6,C4-C5-C6-C1,C5-C6-C1-C2,C6-C1-C2,C3
49	τ_i	N-O	C3(C5)-C4-N9-O13(O14)

*for numbering of atom refer Fig 1

Table 4. Definition of local symmetry coordinates and the value corresponding scale factors used to correct the force fields for CFNB

No.(i)	Symbol[a]	Definition[b]	Scale factors used in calculation
1-6	C-C	r1,r2,r3,r4,r5,r6	0.914
7-9	C-H	S7,S8,S9	0.914
10	C-F	p10	0.992
11	C-Cl	P11	0.992
12	C-N	N12	0.992
13-14	N-O	$\sum_i$13, $\sum_i$14	0.992
15	C-C-C	(α15-α16+α17-α18+α19-α20)/ √6	0.992
16	C-C-C	(2α15-α16-α17+2α18-α19-α20)/ √12	0.992
17	C-C-C	(α16-α17+α19-α20)/2	0.992
18-20	C-C-H	(θ21-θ22)/√2, (θ23-θ24)/√2, (θ25-θ26)/√2	0.916
21	C-C-F	(β27-β28)/√2	0.923
22	C-C-Cl	(Φ29-Φ30)/√2	0.923
23	C-C-N	(μ31-μ32)/√2	0.923
24	C-N-O	(γ33-γ34)/ √2	0.923
25	O-N-O	ν35	0.923
26-28	C-H	ω36, ω37, ω38	0.994
29	C-F	ξ39	0.962
30	C-Cl	Ω40	0.962
31	C-N-O	γ41	0.962
32	C-N	ι42	0.962
33	tring	(τ43-τ44+τ45-τ46+τ47-τ48)/√6	0.994
34	tring	(τ43-τ45+τ46-τ48)/2	0.994
35	tring	(-τ43+2τ44-τ45-τ46+2τ47-τ48)/√12	0.994
36	N-O	τ49/4	0.995

[a] These symbols are used for description of the normal modes by TED in Table 5.
[b] The internal coordinates used here are defined in Table 3.

Table 5. Detailed assignments of fundamental vibrations of CFNB by normal mode analysis based on SQM force field calculation

S. No.	Symmetry species C_s	Observed frequency (cm^{-1})		Calculated frequency (cm^{-1}) with B3LYP/6-311+G ** force field				TED (%) among type of internal coordinates[c]
		Infrared	Raman	Unscaled	Scaled	IR[a] A_i	Raman[b] I_i	
1	A'	3275		3276	3274	8.566	36.542	CH(99)
2	A'		3276	3277	3273	3.936	81.192	CH(99)
3	A'	3247		3245	3243	0.498	106.437	CH(99)
4	A'		1689	1685	1682	126.646	2.234	NOas(58),CC(20),bNO2r(11),bCCN(5)
5	A'	1659		1655	1653	55.881	64.458	CC(67),bCH(14),bring(10),CF(5)
6	A'		1636	1638	1633	82.567	12.304	CC(58),NOas(27),bring(7)
7	A'	1546		1548	1545	100.816	7.186	CC(40),bCH(39),CF(13)
8	A'	1441	1442	1440	1439	13.910	0.187	CC(57),bCH(24),bCCN(5)
9	A'			1399	1398	323.237	177.472	NOss(65),CN(17),bNO2sc(16)
10	A'	1377		1375	1372	15.292	4.919	CC(93)
11	A'		1325	1322	1319	93.890	13.920	CF(47),bCH(23),CC(22),bring(5)
12	A'	1276		1278	1276	2.130	3.210	bCH(73),CC(15)
13	A'		1165	1162	1159	38.639	7.862	bCH(61),CC(24),CCl(6)
14	A'	1148		1146	1144	34.175	21.109	CC(25),CN(23),bring(22),bCH(19)
15	A'		1078	1079	1076	22.797	1.284	bring(30),CC(26),bCH(22),CCl(14)
16	A"	976		978	974	0.379	1.165	gCH(85),tring(12)
17	A"		935	932	929	18.816	0.912	gCH(78),tring(14),gCN(5)
18	A'	926		924	920	26.933	15.207	CC(20),bNO2sc(19),CN(19),bring(16),CCl(10),NOss(7)
19	A"		850	848	846	18.324	2.992	gCH(77),tring(9),gCF(7)
20	A'	828		824	821	3.696	1.547	bNO2sc(38),bring(34),CF(11),CC(9)
21	A"	748	756	754	752	29.793	2.196	gCNO(55),gCN(18),tring(15),gCH(9)
22	A'		721	732	729	61.614	10.142	CCl(27),bring(25),CC(16),bNO2sc(13),CF(6)
23	A"	700		702	697	0.063	0.293	tring(59),gCF(21),gCCl(12)
24	A'		650	648	646	8.486	3.291	bring(63),bNO2sc(9),CN(9),CC(5)
25	A'	568		564	561	1.420	1.966	bNO2r(48),bCCN(17),bCF(10),CC(8),bCCl(7)
26	A"		558	554	550	0.003	0.659	tring(51),gCN(22),gCF(13),gCCl(7)
27	A'	504		502	499	5.104	2.632	bCF(32),bNO2r(20),CCl(15),bCCl(12),bring(11),CC(9)
28	A"		459	456	454	1.759	0.022	tring(62),gCCl(20),gCF(9),gCH(6)
29	A'			372	371	0.163	5.330	bring(44),CCl(16),bCCl(12),bNO2r(11),CC(6)
30	A'			356	354	0.235	3.985	bring(41),CN(30),CC(13),bNO2sc(6)
31	A"		332	337	334	0.546	1.621	tring(27),gCN(24),gCF(19),gCCl(14),gCH(11)
32	A'			261	259	1.103	0.691	bCF(48),bCCl(31),bring(7),bCCN(5)
33	A'		186	180	178	2.479	0.602	bCCN(68),bCCl(17),CC(7)
34	A"			178	176	0.112	1.930	tring(36),gCCl(27),gCN(17),gCH(11),tNO(5)
35	A"		125	120	118	4.078	0.302	tring(61),gCN(17),gCH(15)
36	A"			60	58	0.076	0.377	tNO(86),tring(13)

Abbreviations used: b, bending; g, wagging; t, torsion; s, strong; vs, very strong; w, weak; vw, very weak;

[a] Relative absorption intensities normalized with highest peak absorption

[b] Relative Raman intensities calculated by Eq 1 and normalized to 100.

[c] For the notations used see Table 4.

Table 6. Second order perturbation theory analysis of Fock matrix in NBO basis for CFNB

Donor(I)	Types of Bond	Occupancy	Acceptor(J)	Type of Bond	Occupancy	E(2) Kcal/Mol	E(i)-E(j) a.u.	F(i,j)
C1-C2	σ	1.97605	C1-C6	σ*	0.03662	4.12	1.28	0.065
			C2-C3	σ*	0.01236	2.36	1.31	0.050
			C2-H11	σ*	0.01293	0.96	1.11	0.029
			C3-H12	σ*	0.01332	2.14	1.11	0.044
			C6-Cl7	σ*	0.02768	4.58	0.88	0.057
C1-C6	σ	1.98128	C1-C2	σ*	0.02310	3.44	1.31	0.060
			C2-H11	σ*	0.01293	1.92	1.13	0.042
			C5-C6	σ*	0.02306	3.27	1.32	0.059
			C5-H10	σ*	0.01391	2.08	1.12	0.043
C1-C6	π	1.66058	C2-C3	π*	0.30806	17.31	0.31	0.066
			C4-C5	π*	0.37553	21.60	0.30	0.073
C1-F8	σ	1.99311	C2-C3	σ*	0.01236	1.35	1.40	0.039
			C5-C6	σ*	0.02306	1.68	1.38	0.043
C2-C3	σ	1.96779	C1-F8	σ*	0.03982	4.83	0.85	0.057
			C3-C4	σ*	0.02218	2.78	1.28	0.053

			C4-N9	σ*	0.09752	3.97	1.03	0.058
C2-C3	π	1.65454	C1-C6	π*	0.41243	23.88	0.26	0.072
C2-H11	σ	1.97281	C3-H12	σ*	0.01332	0.55	0.89	0.020
C3-C4	σ	1.97160	N9-O13	σ*	0.03815	1.92	1.36	0.046
C3-H12	σ	1.97465	C1-C2	σ*	0.02310	3.40	1.06	0.054
			C2-C3	σ*	0.01236	0.71	1.09	0.025
			C2-H11	σ*	0.01293	0.58	0.88	0.020
			C3-C4	σ*	0.02218	0.56	1.07	0.022
			C4-C5	σ*	0.37553	4.24	1.07	0.060
C4-C5	σ	1.96490	C6-Cl7	σ*	0.02768	4.35	0.87	0.055
			C3-H12	σ*	0.01332	2.25	1.11	0.045
			C4-N9	σ*	0.09752	0.52	1.04	0.021
			C5-C6	σ*	0.02306	3.24	1.29	0.058
			C5-H10	σ*	0.01391	1.10	1.10	0.031
			N9-O14	σ*	0.09077	2.06	1.04	0.042
C4-C5	π	1.66510	C1-C6	π*	0.41243	18.36	0.28	0.065
			C2-C3	π*	0.30806	21.10	0.30	0.072
			N9-O13	π*	0.52728	15.48	0.20	0.052
C4-N9	σ	1.98743	C2-C3	σ*	0.01236	1.37	1.40	0.039
			C3-C4	σ*	0.02218	1.09	1.39	0.035
			C4-C5	σ*	0.02343	0.84	1.39	0.031
			C5-C6	σ*	0.02306	1.25	1.39	0.037
			N9-O13	σ*	0.03815	0.86	1.46	0.032
C5-C6	σ	1.97136	C1-C6	σ*	0.03662	3.67	1.29	0.062
			C1-F8	σ*	0.03982	4.38	0.87	0.055
			C4-C5	σ*	0.37553	3.23	1.31	0.058
			C4-N9	σ*	0.09752	3.48	1.05	0.055
C5-H10	σ	1.97225	C1-C6	σ*	0.03662	3.93	1.07	0.058
			C3-C4	σ*	0.02218	4.04	1.08	0.059
			C4-N9	σ*	0.09752	1.15	0.82	0.028
C6-Cl7	σ	1.98511	C1-C2	σ*	0.02310	2.35	1.25	0.049
N9-O13	σ	1.99605	C3-C4	σ*	0.02218	0.62	1.81	0.030
			C4-N9	σ*	0.09752	1.57	1.55	0.045
N9-O13	π	1.98910	C4-C5	π*	0.37553	2.65	0.52	0.036
			N9-O13	π*	0.52728	3.47	0.43	0.040
N9-O14	σ	1.99339	C4-C5	σ*	0.02343	0.85	1.48	0.032
			C4-N9	σ*	0.09752	0.51	1.23	0.023
Cl7	LP(1)	1.99297	C1-C6	σ*	0.03662	0.88	1.47	0.032
			C5-C6	σ*	0.02306	1.70	1.48	0.045
	LP(2)	1.96865	C1-C6	σ*	0.03662	4.60	0.85	0.056
			C5-C6	σ*	0.02306	3.71	0.86	0.051
Cl7	LP(3)	1.92158	C1-C6	π*	0.41243	13.22	0.30	0.062
F8	LP(1)	1.99197	C1-C2	σ*	0.02310	1.07	1.64	0.038
			C1-C6	σ*	0.03662	0.84	1.64	0.033
F8	LP(2)	1.97999	C1-C2	σ*	0.02310	3.62	0.94	0.052
			C1-C6	σ*	0.03662	3.79	0.94	0.053
F8	LP(3)	1.94430	C1-C6	π*	0.41243	11.73	0.39	0.066
O13	LP(1)	1.97860	C4-N9	σ*	0.09752	5.11	1.08	0.068
	LP(1)		N9-O14	σ*	0.09077	1.99	1.07	0.042
O13	LP(2)	1.85559	C4-N9	σ*	0.09752	18.12	0.60	0.094
			N9-O14	σ*	0.09077	30.29	0.60	0.122
O14	LP(1)	1.98592	C4-N9	σ*	0.09752	3.55	1.11	0.057
			N9-O13	σ*	0.03815	1.94	1.43	0.047
O14	LP(2)	1.93281	C4-N9	σ*	0.09752	8.72	0.56	0.063
			N9-O13	σ*	0.03815	10.63	0.89	0.087
			N9-O13	π*	0.52728	0.63	0.18	0.011
O14	LP(3)	1.51223	N9-O13	π*	0.52728	93.00	0.17	0.112

Table 7. The dipole moment (μ) and first-order hyperpolarizibility (β) of CFNB derived from DFT calculations

β_{xxx}	**87.442**
β_{xxy}	-524.69
β_{xyy}	-917.17
β_{yyy}	10.215
β_{zxx}	87.756
β_{xyz}	676.71
β_{zyy}	-18.709
β_{xzz}	19.936
β_{yzz}	25.707
β_{zzz}	60.949
β_{total}	1.6578
μ_x	0.58603649
μ_y	0.0944947
μ_z	0.01831499
μ	0.8359702

Dipole moment (μ) in Debye, hyperpolarizibility β(-2ω;ω,ω) 10^{-30}esu.

Table 8. Computed absorption wavelength (λ_{ng}) , energy (E_{ng}), oscillator strength (f_n) and its major contribution

n	λ_{ng}	E_{ng}	f_n	Major contribution
1	262.9	4.72	0.0043	H-6->L+0(+29%)
2	221.7	5.59	0.0047	H-6->L+0(28%), H-3->L+0(+26%)
3	202.6	6.12	0.0222	H-0->L+0(+49%), H-1->L+1(+24%)

(Assignment; H=HOMO,L=LUMO,L+1=LUMO+1,etc.)

The 27 components of the 3D matrix can be reduced to 10 components due to the Kleinman symmetry [18].

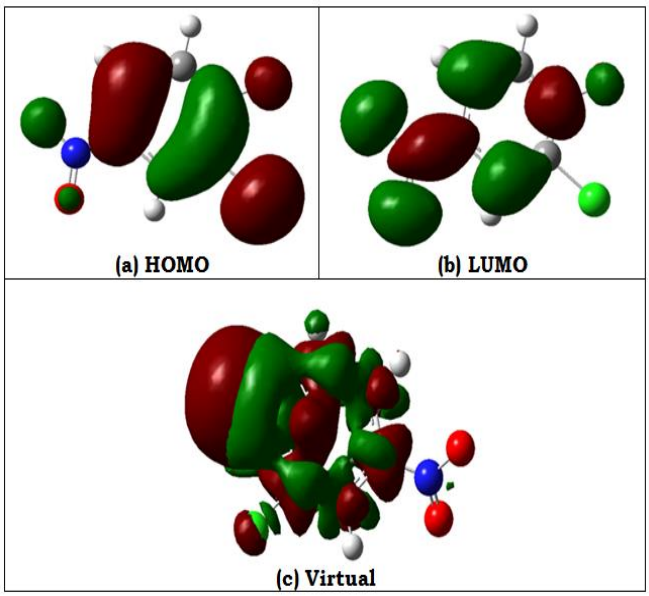

Fig 4. Representation of the orbital involved in the electronic transition for (a) HOMO (b) LUMO (c) Virtual

It can be given in the lower tetrahedral format. It is obvious that the lower part of the 3×3×3 matrixes is a tetrahedral. The components of β are defined as the coefficients in the Taylor series expansion of the energy in the external electric field. When the external electric field is weak and homogeneous, this expansion becomes:

$$E = E^0 - \mu_\alpha F - 1/2\alpha_{\alpha\beta}F_\alpha F_\beta - 1/6\beta_{\alpha\beta\gamma}F_\alpha F_\beta F_\gamma + ...$$

The total static dipole moment is

$$\mu = (\mu_x^2 + \mu_y^2 + \mu_z^2)^{1/2}$$

and the average hyperpolarizability is

$$\beta_0 = (\beta_x^2 + \beta_y^2 + \beta_z^2)^{1/2}$$

and

$$\beta_x = \beta_x + \beta_{xyy} + \beta_{xzz}$$

$$\beta_y = \beta_{yyy} + \beta_{xyy} + \beta_{xzz}$$

$$\beta_x = \beta_x + \beta_{xyy} + \beta_{xzz}$$

TheB3LYP/6-311+G** calculated first-order hyperpolarizability of CFNB is 1.6578x 10^{-30} esu is shown in Table 7.

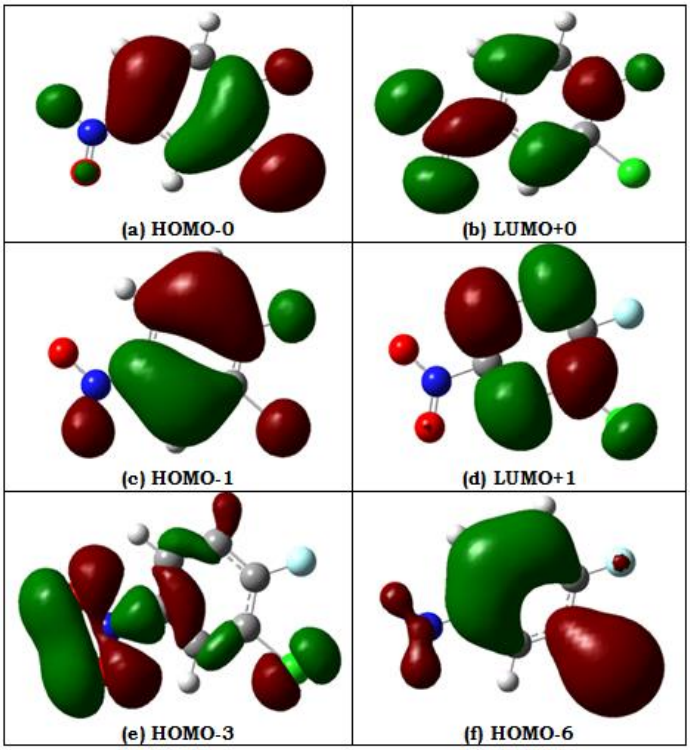

Fig 5. Representation of the orbital involved in the electronic transition for (a) HOMO−0 (b) LUMO+0 (c) HOMO-1 (d) LUMO+1 (e) HOMO-3 (f) HOMO-6

Electronic excitation energies, oscillator strength and nature of the respective excited states were calculated by the

closed-shell singlet calculation method and are summarized in Table 8. Fig 4 shows the highest occupied molecule orbital (HOMO) and lowest unoccupied molecule orbital (LUMO) of CFNB. Orbital involved in the electronic transition for (a) HOMO−0 (b) LUMO+0 (c) HOMO-1 (d) LUMO+1 (e) HOMO-3 (f) HOMO-6 is represented in Fig 5. The NLO responses can be understood by examining the energetic of frontier molecular orbitals. There is an inverse relationship between hyperpolarizability and HOMO–LUMO.

HOMO energy = -0.386 a.u

LUMO energy = 0.040 a.u

HOMO–LUMO energy gap = 0.426 a.u

Conclusions

Based on the SQM force field obtained by DFT calculations at B3LYP/6-311+G** level, the complete vibrational properties of CFNB have been investigated by FT-IR and FT-Raman spectroscopies. The role of fluro, chloro and nitro groups in the vibrational frequencies of the CFNB has been discussed. The various modes of vibrations have unambiguously been assigned based on the results of the TED output obtained from normal coordinate analysis. The assignment of the fundamentals is confirmed by the qualitative agreement between the calculated and observed band intensities (especially with the large basis set) and the results confirm the ability of the methodology applied for interpretation of the vibrational spectra of the title molecules in the solid phase. The stability and intramolecular interactions have been interpreted by NBO analysis and the transactions give stabilization to the structure have been identified by second order perturbation energy calculations. The first-order hyperpolarizabilities (β_0) of this novel molecular system, and related properties β_0, α_0 and $\Delta\alpha$) of CFNB were calculated using B3LYP/6-311+G** basis set, based on the finite-field approach. The first-order hyperpolarizability (β_{total}) of CFNB was calculated and found to be 1.6578×10^{-30} esu. Electronic excitation energies, oscillator strength and nature of the respective excited states were calculated by the closed-shell singlet calculation method. The NLO responses can be understood by examining the energetic of frontier molecular orbitals. There is an inverse relationship between hyperpolarizability and HOMO–LUMO.

References

1. S.J. Cyrin, Molecular Vibrations and Mean Square Amplitudes, Elsevier, Amsterdam, 1968.

2. L.A. Gribov, M.J. Orille-Thomas, Theory and Methods of Calculation of Molecular Spectra, Wiley, Chichester, 1988.

3. M. J. Frisch, G. W. Trucks, H. B. Schlegel, G. E. Scuseria, M. A. Robb, J. R. Cheeseman, G. Scalmani, V. Barone, B. Mennucci, G. A. Petersson, H. Nakatsuji, M. Caricato, X. Li, H. P. Hratchian, A. F. Izmaylov, J. Bloino, G. Zheng, J. L. Sonnenberg, M. Hada, M. Ehara, K. Toyota, R. Fukuda, J. Hasegawa, M. Ishida, T. Nakajima, Y. Honda, O. Kitao, H. Nakai, T. Vreven, J. A. Montgomery, Jr., J. E. Peralta, F. Ogliaro, M. Bearpark, J. J. Heyd, E. Brothers, K. N. Kudin, V. N. Staroverov, R. Kobayashi, J. Normand, K. Raghavachari, A. Rendell, J. C. Burant, S. S. Iyengar, J. Tomasi, M. Cossi, N. Rega, J. M. Millam, M. Klene, J. E. Knox, J. B. Cross, V. Bakken, C. Adamo, J. Jaramillo, R. Gomperts, R. E. Stratmann, O. Yazyev, A. J. Austin, R. Cammi, C. Pomelli, J. W. Ochterski, R. L. Martin, K. Morokuma, V. G. Zakrzewski, G. A. Voth, P. Salvador, J. J. Dannenberg, S. Dapprich, A. D. Daniels, O. Farkas, J. B. Foresman, J. V. Ortiz, J. Cioslowski, and D. J. Fox, Gaussian, Inc., Wallingford CT, 2009.

4. A.D. Becke, J. Chem. Phys., 98 (1993) 5648.

5. C. Lee, W. Yang, R.G. Parr, Phys. Rev., B37 (1988) 785.

6. T. Sundius, J. Mol. Struct. 218 (1990) 321.

7. A. Frisch, A.B. Nielson, A.J. Holder, Gaussview Users Manual, Gaussian Inc., Pittsburgh, PA, 2000.

8. G. Keresztury, S. Holly, J. Varga, G. Besenyei, A.V. Wang, J.R. Durig, Spectrochim. Acta 49A,2007 (1993).

9. G. Keresztury, in: J.M. Chalmers and P.R. Griffiths(Eds), Handbook of Vibrational Spectroscopy vol.1, John Wiley & Sons Ltd. p. 71, (2002).

10. P. Pulay, G. Fogarasi, F. Pong, J.E. Boggs, J. Am. Chem. Soc.,101 (1979) 2550.

11. V. Krishnakumar, V. Balachandran, Spectrochim. Acta 63A (2006) 464−476.

12. K. Furic, V. Mohacek, M. Bonifacic, I. Stefanic, J. Mol. Struct. 267 (1992) 39−44.

13. V.K. Rastogi, M. Alcolea Palafox, Rashmi Tomar and Upama Singh, Spectrochimica Acta Part A: Molecular and Biomolecular Spectroscopy, 110 (2013) 458-470.

14. B. Lakshmaiah, G. Ramana Rao, J. Raman Spectrosc. 20 (1989) 439.

15. M. Arivazhagan and S. Jeyavijayan, Spectrochimica Acta Part A: Molecular and Biomolecular Spectroscopy, 79 (2011) 376-383.

16. L.J. Bellamy, R.L. Williams, Spectrochim. Acta A (1957) 341−345.

17. V. Karunakaran and V. Balachandran, Spectrochimica Acta Part A: Molecular and Biomolecular Spectroscopy, 98 (2012) 229-239.

18. D.A. Kleinman, Phys. Rev. 1962;126,1977.